Hypertonic saline improves brain edema resulting from traumatic brain injury by suppressing the NF-κB/IL-1β signaling pathway and AQP4

HUI ZHANG*, JUN LIU*, YUNZHEN LIU, CHUNHAI SU, GAOYANG FAN, WENPENG LU and LEI FENG

Department of Neurosurgery, Jining No. 1 People's Hospital, Jining, Shandong 272111, P.R. China

Received September 4, 2019; Accepted April 17, 2020

DOI: 10.3892/etm.2020.9199

Abstract. Although hypertonic saline (HS) has been extensively applied to treat brain edema in the clinic, the precise mechanism underlying its function remains poorly understood. Therefore, the aim of the present study was to investigate the therapeutic mechanism of HS in brain edema in terms of aquaporins and inflammatory factors. In the present study, traumatic brain injury (TBI) was established in male adult Sprague-Dawley rats, which were continuously administered 10% HS by intravenous injection for 2 days. In addition, brain edema and brain water content were detected by MRI and wet/dry ratio analysis and histological examination, respectively. Immunohistochemical staining for albumin and western blotting for occludin, zonula occludens-1 and claudin-5 was performed to evaluate the integrity of the blood-brain barrier. Aquaporin 4 (AQP4) expression was also analyzed using western blotting and reverse transcription-quantitative PCR, whilst interleukin (IL)-1β and NF-κB levels were measured using ELISA. It was demonstrated that HS treatment significantly reduced brain edema in TBI rats and downregulated AQP4 expression in cerebral cortical tissues around the contusion site. In addition, IL-1β and NF-κB levels were found to be downregulated after 10% HS treatment. Therefore, results from the present study suggested that HS may protect against brain edema induced by TBI by modulating the expression levels of AQP4, NF-κB and IL-1β.

Introduction

Brain edema is a common complication following traumatic brain injury (TBI) around the world, which is associated with high disability, mortality and morbidity rates. In 2014, the Centers for Disease Control and Prevention documented 2.53 million TBI-related emergency department visits and there were approximately 288,000 TBI-related hospitalizations and 56,800 TBI-related deaths (1). As a result, it severely affects the physical and mental wellbeing of patients (2). In addition, brain edema is an important secondary pathophysiological reaction following severe cerebral trauma, which is characterized by the pathological excessive water accumulation in spaces inside and outside brain cells and an enlarged brain volume (3). This in turn induces and aggravates intracranial hypertension. In some severe cases, it may induce brain shift and cerebral hernia, which are major factors leading to disability and mortality (4). Although dehydration remains to be the major treatment option for brain edema, the pathogenesis of traumatic brain edema is highly complex and is generally induced by the combined action of multiple factors, including disturbances in the microcirculation and the blood-brain barrier (BBB), disorder of brain cell energy metabolism, oxygen free radical damage, excitatory amino acid poisoning, calcium ion overload, nitric oxide damage, lactic acidosis and monoamine neurotransmitter toxicity (5). In recent years, aquaporin 4 (AQP4) and the inflammatory response, which have been reported to participate in the pathogenesis and therapeutic mechanism of brain edema, have attracted increasing attention (6).

The AQP family consists of water channel proteins that participate in water homeostasis regulation (7). It consists of 13 members (AQP1-13) that are conserved across mammalian species, among which 7 (AQP1, 3, 4, 5, 8, 9 and 11) can be detected in the central nervous system (CNS) (8). AQP4 is mostly expressed in astrocytes and is the water channel with the highest abundance in brain, which serves a vital role in water and ion homeostasis (9). In addition, AQP4 has also been widely suggested to exert a central and multifunctional role in brain edema formation (6). In a previous study, AQP4-deficient mice were not found to differ from wild-type mice in terms of brain morphology and other physiological functions in a previous study (10). However, during pathological processes such as fluid infusion into the parenchyma, focal frozen injury of the cortex and the implantation of melanoma cells, AQP4-deficient mice exhibited increased severe brain swelling compared with that in wild-type mice (10). However, a recent study by Yao *et al* (11) found that, AQP4 knockout

Correspondence to: Dr Lei Feng, Department of Neurosurgery, Jining No. 1 People's Hospital, 6 Jiankang Road, Jining, Shandong 272111, P.R. China
E-mail: jnfenglei@sina.com

*Contributed equally

Key words: brain edema, hypertonic saline, aquaporin 4, NF-κB, interleukin-1β, blood-brain barrier

has been previously demonstrated to reduce the infarct volume and brain edema, to provide a neuroprotective effect in mice with permanent middle cerebral artery occlusion (11). AQP4 has also been reported to be associated with inflammation, where AQP4 downregulation could downregulate inflammatory cytokines, including interleukin (IL)-6, IL-1β, tumor necrosis factor (TNF)-α and IL-10, which can protect neonatal rats from brain edema induced by hypoxia-ischemia (12). In addition, a previous study revealed that 3% hypotonic saline (HS) can reduce brain edema resulting from TBI by downregulating TNF-α and AQP4, reducing cell apoptosis (13). However, the effect of AQP4 on HS-mediated protection from traumatic brain edema, the related mechanism and the regulatory mechanism of the inflammatory response are not fully understood. Therefore, the aim of the present study was to assess the effect of HS on TBI-induced brain edema and the associated inflammatory response using a rat model.

Materials and methods

Animals and TBI model. A total of 60 adult male Sprague-Dawley (SD) rats (weight range, 220-270 g, 7 weeks old) were provided by Beijing Vital River Laboratory (Beijing, China). Animal treatments and experiments were carried out in accordance with the 'Guide for the Care and Use of Laboratory Animals' of the National Institutes of Health (14). The present research protocol was approved the Institutional Animal Care and Use Committee of Jining No. 1 People's Hospital (Jining, China). Each rat was maintained in an individual cage with free access to water and food and allowed 1 week of adaptive feeding at 24˚C and relative humidity of 55-65% on a normal light cycle (12/12-h, lights on from 7:00 a.m. to 7:00 p.m.) prior to experimental surgery to minimize animal suffering.

A controlled cortical impact model of TBI was induced *in vivo* in rats as described previously (15). Animals were anesthetized by isoflurane inhalation (4% for induction and 1.8% for maintenance) mixed with pure oxygen at a flow rate of 500 ml/min (cat. no. R630; Shenzhen Ruiwode Life Technology Co., Ltd.); animals were maintained at 37±0.5˚C throughout the operation using thermal mats. Rats were placed on a stereotaxic frame and secured with an incisor bar and two ear bars. Subsequently, a craniotomy (diameter, 5 mm) was performed on the right parietal cortex (3 mm lateral and posterior from Bregma) with a dental drill. Disruption of the dura and the associated vasculature was avoided as much as possible during the process of craniotomy. A PCI 3000 PinPoint Precision Cortical Impactor (Hatteras Instruments, Inc.), equipped with an impactor tip (diameter, 4 mm), was used to deliver an impact at a velocity of 4.5 m/sec. the dwell time was 75 msec and the deformation was 1 mm. Following the induction of TBI, the piece of resected skull was immediately replaced and secured with bone wax. The incision was then closed using interrupted 4-0 silk stitches. An identical procedure with the exception of impact delivery was performed on sham rats.

Experimental procedure. Rats were randomized into three groups: i) Sham group (n=18); ii) vehicle-treated TBI group (n=21); and iii) HS-treated TBI group (n=21). For HS treatment, animals were given an intravenous injection of 10% HS (10 g NaCl in 100 ml deionized water) via the tail vein (0.08 ml/g; infusion rate, 0.3 ml/h) 3 h after the induction of TBI (16,17). For vehicle-treated rats, an equivalent amount of normal saline (0.9 g NaCl in 100 ml deionized water) was infused intravenously. The rats were sacrificed 2 days after treatment for further analyses.

MRI. Sequential MRI was conducted in 21 rats (including 5, 8 and 8 from the sham, HS-treated and vehicle-treated groups, respectively) at 0 and 48 h after TBI using a 7.0 T scanner (BioSpec Products, Inc.) equipped with a four-channel phased array rat head coil.

T2-weighted turbo spin-echo images (T2WI) were obtained using the fast spin-echo sequence (under conditions of field-of-view, 35x35 mm; matrix, 256x256; number of scans, 20; slice thickness, 1 mm; echo time, 33 msec; repetition time, 2838.2 msec; number of averages, 1). The obtained images were analyzed using the OsiriX software (version 4.2.2; http://www.osirix-viewer.com). To quantify the size of the lesion on T2WI, both the brain and lesion areas were delineated on a single slice by two researchers who reached a consensus, where the region of interest defined by the researchers on each slice containing the lesion was used. The brain and lesion volumes were summed for all animals.

Over the course of TBI, the contralateral brain area was determined according to the aforementioned method and was also delineated in the obtained images in accordance with rescaled drawings from the Paxinos and Watson Atlas (18). Hyperintense pixels in the ipsilateral cortex on the T2WI were regarded as significantly higher signals ($P<0.05$) compared with those in the contralateral hemisphere. Additionally, lesion volume on the T2WI (Vu) was calculated by multiplying the slice thickness by the hyperintense area on each slice. To compensate for the effect of brain swelling, the adjusted brain swelling (swelling %) and lesion volume (Ve %), which were presented in the form of volume increases in the affected hemisphere, were computed according to the equation below (19):

$$Ve = Vc + Vi - (Vc + Vi - Vu)\frac{Vc + Vi}{2Vc}$$

$$\text{swelling } \% = \frac{2(Ve - Vu)}{Vc + Vi} \times 100$$

where Vu and Ve represent the uncorrected and corrected lesion volumes, respectively and Vc and Vi represent the contralateral and ischemic hemisphere volumes, respectively.

Neurological deficit tests. The modified neurological severity score (mNSS) of each group was evaluated at 48 h following TBI in a blinded manner according to a previously described method (20). Neurological function scores ranged from 0-18, with a higher score indicating a more severe injury (20).

Hematoxylin and eosin (H&E) and immunohistochemical (IHC) staining. Coronal sections of the cerebral cortical tissues around the contusion site were selected for H&E and IHC staining. Rats were sacrificed and perfused with PBS via the left ventricle followed by 4% paraformaldehyde for fixation. Then, the collected cerebral tissues were fixed at room temperature in buffered paraformaldehyde (4%) for 24 h embedded in paraffin and sectioned into 4-μm slices. H&E

staining was performed after deparaffinization by xylene followed by a descending ethanol gradient at room temperature, where the stained tissues were examined under a light microscope (magnification, x400).

For IHC staining, rats were sacrificed and perfused with PBS via the left ventricle followed by 4% paraformaldehyde for fixation. Cortical tissues around the contusion site were collected and fixed at room temperature in 4% buffered paraformaldehyde for 24 h embedded in paraffin and sectioned into 4-μm slices, which were then deparaffinized using xylene and rehydrated by descending ethanol gradient. Hydrogen peroxide (3%) was diluted with deionized water and used to block endogenous peroxidase activity for 10 min at room temperature. Slices were incubated in citrate buffer (at pH=6.0) for 10 min at 98˚C for antigen retrieval and incubated with 10% goat serum (cat. no. ZLI-9022; Origene Technologies, Inc.) blocking solution for 20 min at 37˚C. Subsequently, the slices were incubated with the following primary antibodies: Rabbit anti-rat glial fibrillary acidic protein (GFAP; 1:2,000; cat. no. Z0334; Dako; Agilent Technologies, Inc.), chicken anti-rat albumin (1:1,000; cat. no. ab106582; Abcam) and rabbit anti-AQP4 (1:1,000; cat. no. ab128906; Abcam), overnight at 4˚C. The slices were then washed twice with PBS and then incubated at 37˚C with the relevant polymeric horseradish peroxidase (HRP)-labeled anti-rabbit immunoglobulin G secondary antibody (Super Vision IHC kit; cat. no. SV0002; Boster Biological Technology) for 30 min at 37˚C. After staining with 3,3'-diaminobenzidine for ~3 min at room temperature, all slices were counterstained with hematoxylin for 2 min at 37˚C, dehydrated and mounted on coverslips for light microscopic examination. IHC staining for albumin, GFAP and AQP4 was examined by ImageJ software 1.8.0 (National Institutes of Health). In total, six visual fields from each slice (magnification, x400) were examined and the average optical density (OD) was determined for all images.

Determination of brain water content (BWC). Brain edema was evaluated by calculating the BWC of all animals according to a previously described method (21). The dry and wet weights of the brain were determined, where the water content was calculated for all samples based on the following equation: 100% x [(wet weight - dry weight)/wet weight].

Blood sodium concentration assay. Before the experiment ended, a 1-ml blood sample was collected from the rat tail vein under anesthesia as described previously (22). Blood sodium concentration was analyzed immediately using an ABL80 type automatic blood gas system (Radiometer Medical Ltd.) by another technician blinded to the experimental groups.

ELISA. The plasma level of IL-1β was determined using ELISA. Blood samples (1 ml) were collected from the rat abdominal aorta under anesthesia as aforementioned and then subjected to 15 min centrifugation at 800 x g at 4˚C. The plasma IL-1β concentration was measured using a commercial ELISA kit (cat. no. F15810, Shanghai Xitang Biological Technology Co., Ltd.) in accordance with the manufacturer's protocol. Then, the OD at 450 nm was determined using a microplate reader.

Reverse transcription-quantitative PCR (RT-qPCR). Total RNA was isolated from cells and brain tissue from the area surrounding the edema using RNAiso plus (cat. no. 9109; Takara Biotechnology Co., Ltd.). RNA quantification was carried out using a spectrophotometer (NanoDrop 2000; PEQLAB Biotechnologie GmbH), and cDNA was synthesized from 1.0 μg RNA by reverse transcriptase M-MLV (cat. no. 2641; Takara Biotechnology Co., Ltd.) according to manufacturer's protocol. The temperature and duration for reverse transcription was as follows: 42˚C for 10 min and 95˚C for 2 min. The primer sequences used for RT-PCR were as follows: NF-κB forward, 5'-ACAGCCTGGTAGTGCGGTCGT-3' and reverse, 5'-TCAGCAAGTGGCTAGTCTGT-3'; IL-1β forward, 5'-AAAAGCTTGGTGATGTCTGG-3' and reverse, 5'-TTTCAACACGCAGGACAGG-3'; AQP4 forward, 5'-CTTTCTGGAAGGCAGTCTCAG-3' and reverse, 5'-CCACACCGAGCAAAACAAAGAT-3'; and GADPH (the reference gene), forward, 5'-CGGATTTGGTCGTATTGGG-3' and reverse, 5'-CTGGAAGATGGTGATGGGATT-3'. qPCR was performed with SYBR® Premix Ex™ Taq (Takara Biotechnology Co., Ltd) using an ABI 7500 RT PCR System (Applied Biosystems; Thermo Fisher Scientific, Inc.). The thermocycling conditions were as follows: 95˚C for 10 sec, followed by 40 cycles of 95˚C for 5 sec and 60˚C for 30 sec. A dissociation curve was used to examine the detected signal specificity, which constituted a single peak. The $2^{-\Delta\Delta Cq}$ method was used for quantification of expression (23).

Western blotting. The perilesional brain tissue was isolated from each treatment group 2 days following TBI, which was subjected to homogenization with cytoplasmic buffer supplemented with KCl (10 mM), HEPES (10 mM, at pH=7.9), EGTA (0.1 mM), EDTA (0.1 mM), Nonidet P-40 (0.15%), DTT (1 mM), NaF (10 mM), β-glycerophosphate (50 mM), and Na_3VO_4 (5 mM) and phosphatase inhibitors (Roche Diagnostics). The homogenates were subjected to 30 min centrifugation at 12,000 x g at 4˚C, following which the supernatant was discarded and the pellet was not disturbed. To extract nuclear protein, a nuclear buffer was supplemented with NaCl (400 mM), HEPES (20 mM, at pH=7.9), EGTA (1 mM), EDTA (1 mM), Nonidet P-40 (0.50%), DTT (1 mM), NaF (10 mM), Na_3VO_4 (5 mM), β-glycerophosphate (50 mM), in addition to the protease inhibitor cocktail and the buffer was added to the aforementioned pellet. Subsequently, the homogenates were subjected to a further 15 min incubation on ice after vortexing at room temperature for 20 sec, which was repeated four times. The homogenates were then subjected to 15 min of centrifugation at 12,000 x g at 4˚C to assess the nuclear NF-κB.

AQP4 expression was measured using total protein extracts. Protein was collected from brain tissues around the injury site using a total protein extraction kit (Bei Jing Pu Li Lai Gene Technology Co., Ltd.) in accordance with the manufacturer's protocol. Then, the resultant homogenates were subjected to 30 min of centrifugation at 12,000 x g at 4˚C and the supernatants were collected to analyze the amount of total protein extracted using a bicinchoninic acid protein assay kit (cat. no. P0012S; Beyotime Institute of Biotechnology). Protein lysates (20 μg) were subjected to 15 min of denaturation at 90˚C and 10% SDS-PAGE was performed before the proteins

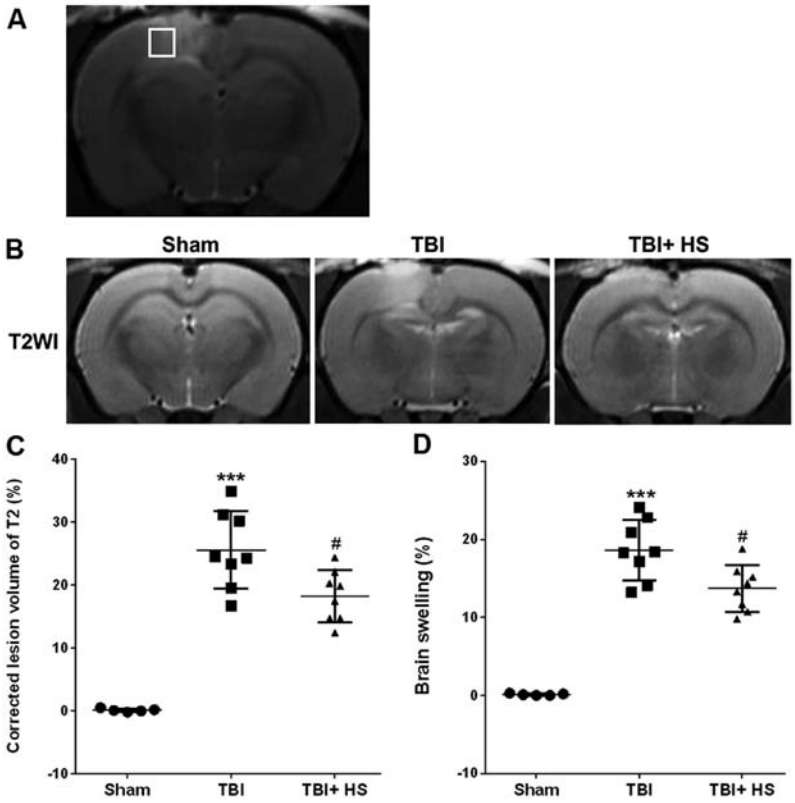

Figure 1. HS treatment reduces the TBI-induced lesion volume and cerebral swelling according to the T2WI. (A) White frame in the T2WI shows the brain region examined in the current study. (B) Representative T2WI of rats in the sham, vehicle-treated and HS-treated rat groups captured 2 days after TBI. (C) Quantitative analysis of the corrected lesion volume using the T2WI of each group 2 days after TBI. (D) Quantitative analysis of brain swelling using the T2WI 2 days following TBI. Data are presented as the mean ± SD. ***P<0.001 vs. Sham group; $^{\#}$P<0.05 vs. TBI group. TBI, traumatic brain injury; T2WI, T2-weighted image; HS, hypertonic saline.

were transferred onto PVDF membranes (EMD Millipore). Subsequently, the membranes were subjected to 2 h blocking using 5% non-fat milk at 37˚C and incubated overnight at 4˚C with primary antibodies, including anti-NF-κB (1:1,000; cat. no. 8242; Cell Signaling Technology, Inc.), anti-AQP4 (1:800; cat. no. ab46182; Abcam), anti-zonula occludens-1 (ZO-1; 1:400; cat. no. 61-7300; Invitrogen; Thermo Fisher Scientific, Inc.), anti-claudin-5 (1:1,000; cat. no. 35-2500; Invitrogen; Thermo Fisher Scientific, Inc.), anti-occludin (1:400; cat. no. 33-1500; Invitrogen; Thermo Fisher Scientific, Inc.), anti-GAPDH (1:1,000; cat. no. AF1186; Beyotime Institute of Biotechnology) and anti-Histone H3 (1:1,000; cat. no. AH433; Beyotime Institute of Biotechnology). Then, the membranes were rinsed with PBST containing 0.1% Tween-20 for 10 min and repeated five times. Subsequently, the PVDF membranes were incubated with a HRP-labeled goat anti-rabbit IgG (1:5,000; cat. no. abs20002; Absin Biotechnology Co., Ltd.) or HRP-labeled goat anti-mouse IgG secondary antibody (1:5,000; cat. no. abs20001; Absin) at 25˚C for 1 h. The bands were visualized using the ECL (cat. no. P0018; Beyotime Institute of Biotechnology) method and analyzed with the ImageJ software 1.8.0 (National Institutes of Health). GAPDH was used to normalize the expression of the proteins, whilst histone H3 was used to normalize the expression of NF-κB in the nuclear extracts.

Statistical analysis. Each value was measured three times and data are presented as the mean ± SD. SPSS 18.0 (IBM Corp.) was used for statistical analyses. No repeated-measure (matched) values were available in the current study, and all of the values were examined by one-way ANOVA and Tukey's post hoc test. P<0.05 was considered to indicate a statistically significant difference.

Results

HS treatment reduces the volume of TBI-induced lesions on T2WI. MRI was first performed to determine the efficacy of HS treatment on lesions induced by TBI, as observed on the T2WI (Fig. 1A). On day 3 following TBI, the corrected T2WI Ve were found to be 18.25±4.13 and 25.59±6.13% in the HS and vehicle groups, respectively (P<0.05; Fig. 1B and C). In addition, HS treatment significantly alleviated brain swelling compared with that in the vehicle group, where the HS and vehicle groups exhibited values of 13.73±2.98 and 18.63±3.87%, respectively (P<0.05; Fig. 1D).

HS improves TBI-induced neurological functional deficits and brain edema. Compared with the sham group, the mNSS scores of the TBI group were found to be significantly increased at 48 h post-TBI. HS treatment significantly reduced the mNSS scores compared with those of TBI alone, suggesting that HS significantly reduced neurological deficits (P<0.05; Fig. 2A). Subsequently, TBI-induced brain edema was evaluated by measuring the BWC, where it was demonstrated that the BWC was significantly increased in

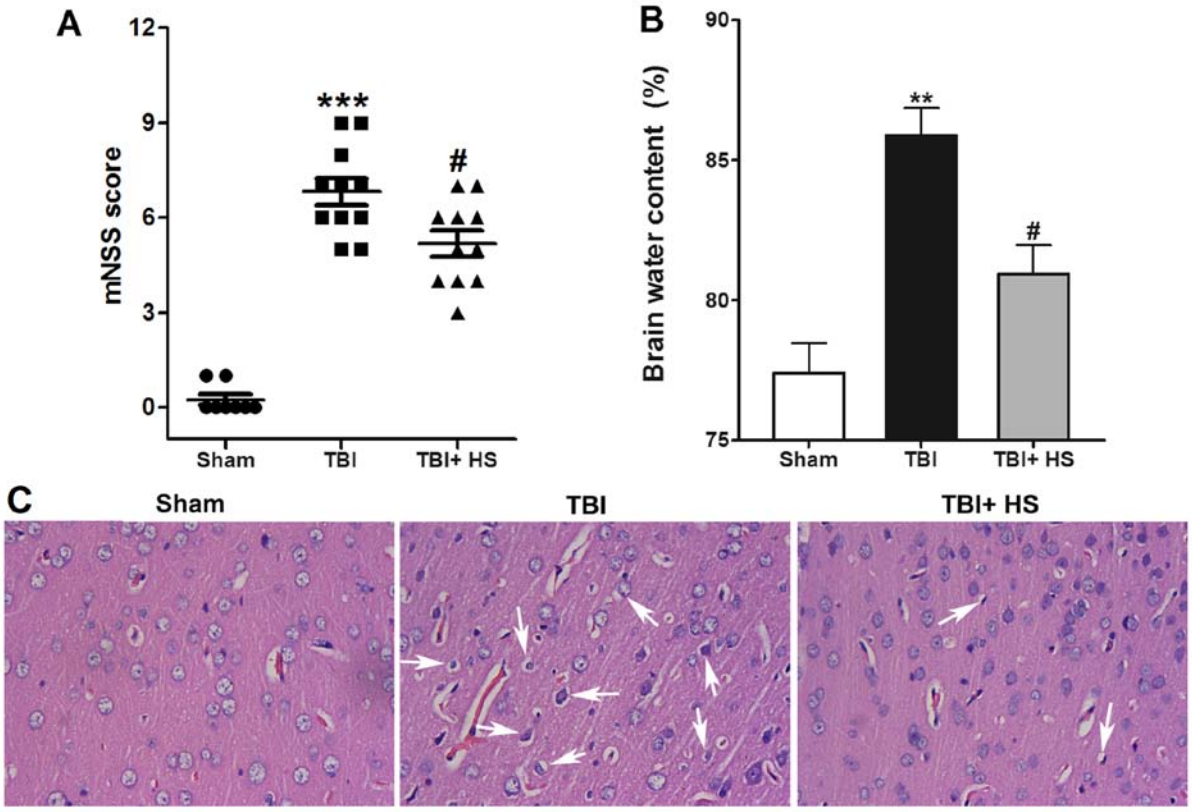

Figure 2. HS improves TBI-induced neurological functional deficits and brain edema. (A) HS treatment significantly reduced neurological deficits at 48 h post-TBI. (B) Brain water content was measured in each rat from the sham, TBI and TBI + HS treatment groups to evaluate brain edema. (C) Representative hematoxylin and eosin staining images identified that TBI-induced pyknotic and shrunken nuclei, and cellular edema, which were ameliorated by HS treatment. White arrows indicate the injured cells with pyknotic or shrunken nuclei induced by cellular edema. Magnification, x400. Data are expressed as the mean ± SD. $^{\#}$P<0.05 vs. TBI group. **P<0.01 vs. the sham group. TBI, traumatic brain injury; HS, hypertonic saline; mNss, modified neurological severity score.

the ipsilateral cortex in the TBI group compare with that in the sham group, which was significantly reversed by HS treatment (Fig. 2B).

H&E staining results identified a regular arrangement of neurons in the sham group, along with capillary morphogenesis and normal glial cells. However, 2 days following TBI, the majority of cells were disorderly arranged where the nuclei became pyknotic or were severely shrunken. In addition, cellular swelling and hypervacuolization were observed in certain areas. HS treatment significantly improved TBI induced nuclei shrinking and cell swelling (Fig. 2C).

HS improves TBI-induced BBB injury. BBB leakage was next assessed by IHC staining for albumin and western blotting for claudin-5, ZO-1 and occludin. It was found that albumin staining was largely negative in the sham group, whilst a significant increase in albumin expression was observed in tissues from the TBI group (Fig. 3A and B), indicating BBB injury. Albumin expression was found to be significantly downregulated in tissues in the HS group compared with that in the TBI group alone.

In addition, tight junction (TJ)-associated proteins, including occludin, ZO-1 and claudin-5, were also revealed to be significantly downregulated by TBI, which was significantly reversed by HS treatment (Fig. 3D). Therefore, these results suggested that HS treatment alleviated BBB destruction following TBI.

HS reduces TBI-induced astrocyte activation. Astrocyte activation was evaluated by IHC staining for GFAP (Fig. 4). GFAP expression was detected in the sham group, which identified few astrocytes with finely branched protrusions. In the TBI group, GFAP expression was demonstrated to be elevated with astrocyte hyperplasia, cell body enlargement, protrusions, thickening and extravascular collagen fibers all observed, suggesting the activation of astrocytes. However, after HS treatment, GFAP expression remained to be elevated compared with that in the sham group, but was significantly lower compared with that in the TBI group, suggested that the astrocyte protrusions did not completely recover their fine morphology. Therefore, it was speculated that HS mitigated astrocyte activation around the site of TBI.

AQP4 expression is reduced by HS treatment. AQP4 expression tissues around the contusion site was evaluated using IHC (Fig. 5). A small amount of AQP4 expression was observed in the sham group, which was significantly upregulated in the TBI group, where AQP4 staining was clearly observed around the blood vessels. After HS treatment, AQP4 expression was significantly downregulated compared with that in the TBI group, where the positively stained particles were substantially smaller.

AQP 4 expression in peri-TBI tissues was also measured using western blotting and RT-qPCR. Compared with the sham group, the protein and mRNA expression levels of AQP4

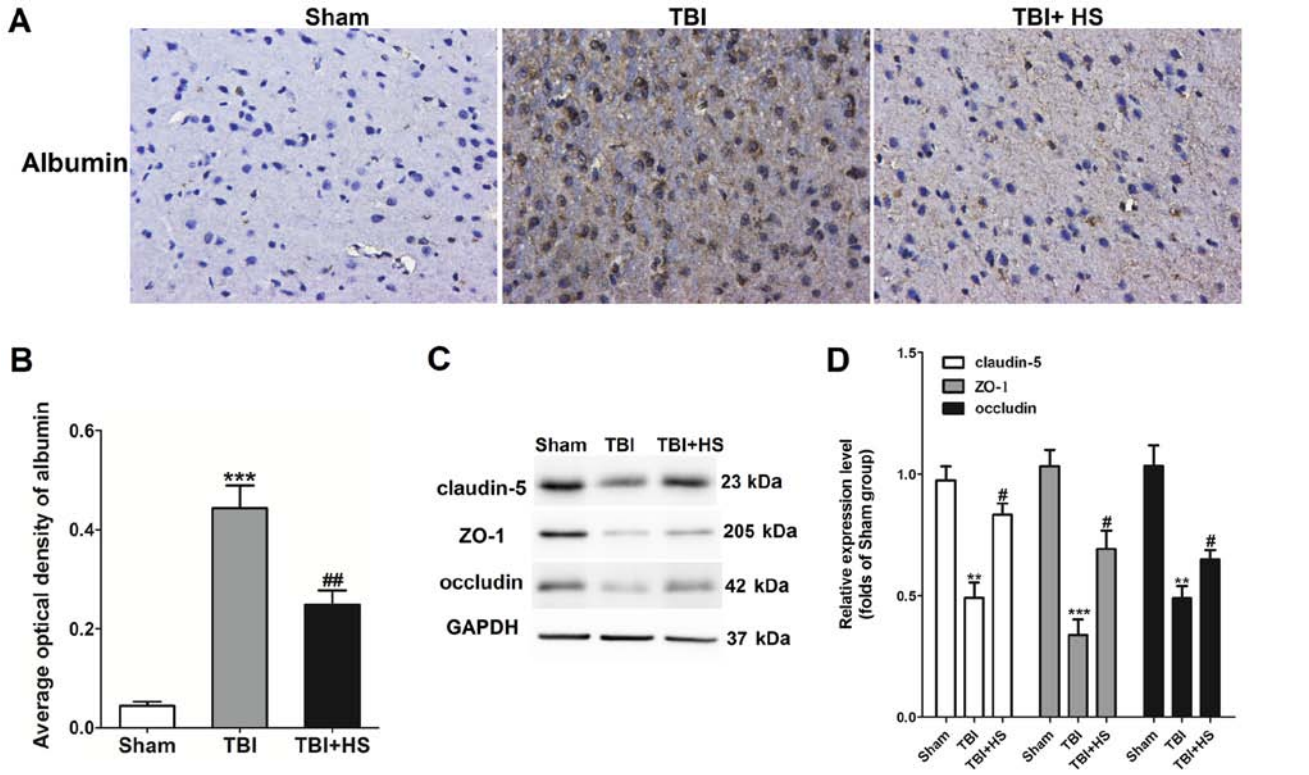

Figure 3. HS improves TBI-induced BBB injury. (A) BBB integrity was evaluated by immunohistochemical staining for albumin. Magnification, x400. (B) Average optical density of albumin staining from the three treatment groups. (C) Expression levels of occludin, ZO-1 and claudin-5 were evaluated by western blotting and (D) Quantified. Data are presented as the mean ± SD. $^{\#}$P<0.05 and $^{\#\#}$P<0.01 vs. TBI group. **P<0.01, ***P<0.001 vs. the sham group. TBI, traumatic brain injury; HS, hypertonic saline; BBB, blood brain barrier; ZO-1, zonula occludens-1.

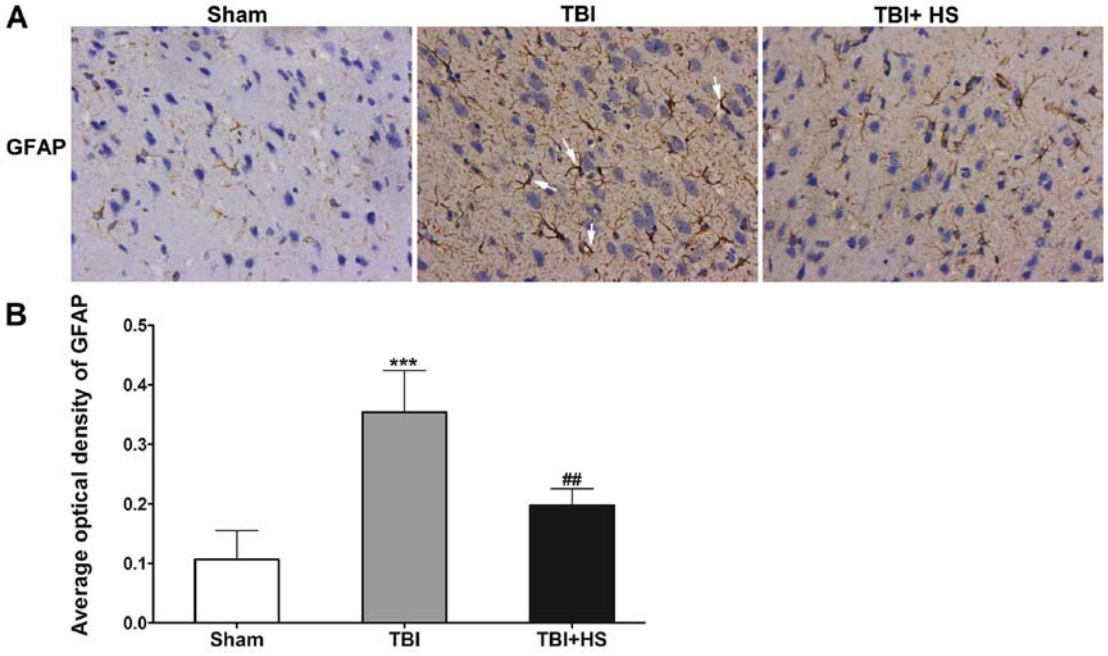

Figure 4. HS reduces TBI-induced astrocyte activation. (A) Astrocyte activation was evaluated by immunohistochemical staining for GFAP. Magnification, x400. TBI increased the expression of GFAP along with astrocyte hyperplasia, cell body enlargement, protrusion and thickening, as well as extravascular collagen fibers, which were ameliorated by HS treatment. White arrows indicate the thickening extravascular collagen fibers. (B) Average optical density of GFAP staining. Data are presented as the mean ± SD. $^{\#\#}$P<0.01 vs. TBI group. ***P<0.001 vs. sham group. TBI, traumatic brain injury; HS, hypertonic saline; GFAP, glial fibrillary acidic protein.

in the TBI group were found to be markedly increased, which was reversed by HS treatment.

Detection of inflammatory factors. The blood sodium concentration was analyzed using an automatic blood gas

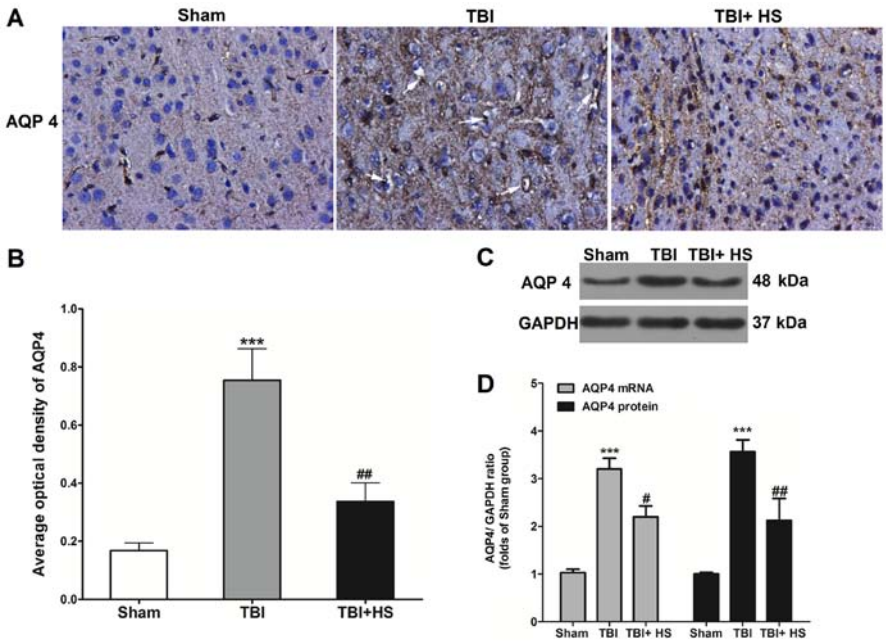

Figure 5. HS treatment reduces AQP4 expression in cerebral cortical tissues around the contusion site. (A) Representative images of immunohistochemical staining for AQP4 indicated that TBI-induced AQP4 upregulation was ameliorated by HS treatment. White arrows indicate the AQP4 positive staining around the blood vessels. Magnification, x400. (B) Average optical density of AQP4 staining. (C) Western blotting and (D) reverse transcription-quantitative PCR were utilized to detect the mRNA and protein expression levels of AQP4 in each group 2 days after TBI. Data are presented as the mean ± SD. $^{\#}$P<0.05, $^{\#\#}$P<0.01 vs. TBI group. ***P<0.001 vs. the sham group. TBI, traumatic brain injury; HS, hypertonic saline; AQP4, aquaporin 4.

Table I. Blood sodium concentrations in each treatment group.

Treatment group	Sodium concentration, mmol/l
Sham	144.50±0.94
TBI	149.75±1.33
TBI + HS	158.11±2.2[a]

[a]P<0.05 vs. Sham. TBI, traumatic brain injury; HS, hypertonic saline.

system, where the results showed that HS treatment remarkably increased the blood sodium ion concentration from 144.50±0.94 mmol/l (sham group) to 158.11±2.2 mmol/l (P<0.05; Table I).

The expression levels of inflammatory factors in each group were next measured (Fig. 6). Western blotting and RT-qPCR results suggested that, compared with the sham group, the protein and mRNA expression levels of NF-κB in the TBI group were significantly higher whilst HS treatment significantly reduced NF-κB expression compared with those in the TBI group.

Serum IL-1β levels were next measured using ELISA. Compared with the sham group, the serum IL-1β level in the TBI group was found to be significantly higher, which was significantly reversed by HS treatment. RT-qPCR was also performed in the tissue samples to detect the changes in IL-1β mRNA expression. Compared with the sham group, IL-1β mRNA expression in the TBI group was significantly higher, but HS treatment significantly downregulated IL-1β expression compared with that in the TBI group.

Discussion

HS has previously demonstrated efficacy in treating brain edema in the clinic, but the precise underlying mechanism remains unknown. In the present study, MRI was performed to investigate the effects of HS on brain edema induced by TBI in rats. It was demonstrated that HS treatment significantly reduced the degree of brain edema in rats, restored the integrity of the BBB, reduced the activation of astrocytes and downregulated AQP4 expression. In addition, detection of inflammatory factors indicated that HS significantly reduced IL-1β and NF-κB expression.

AQP4 is the most important isoform of aquaporin in mammalian brain tissues, which regulate brain water homeostasis and has been previously demonstrated to be closely correlated with the formation of traumatic brain edema (6). Brain edema is related to AQP4 in astrocytes peripheral to the BBB (24). Previous studies on brain edema have focused on the balance between brain tissues and serum osmotic pressure, where a reduction in serum osmotic pressure results in a concentration gradient that induces brain edema (25,26). However, it has been reported that edemas mainly form in the astrocyte foot processes in capillaries instead of neurons (27). In addition, AQP4 is mainly expressed in only astrocytes and not neurons (28). Therefore, AQP4 represents an important target for treating brain edema. A previous study reported that AQP4 expression in astrocytes is increased under numerous pathological conditions in which cytotoxic edema serves a dominant role, including TBI, stroke, meningitis and hyponatremia (29). Appelboom *et al* (30) showed that the severity of brain edema formed due to brain tissue hemorrhage is associated with the AQP4 gene. Additionally, Suzuki *et al* (31) found that both protein and mRNA expres-

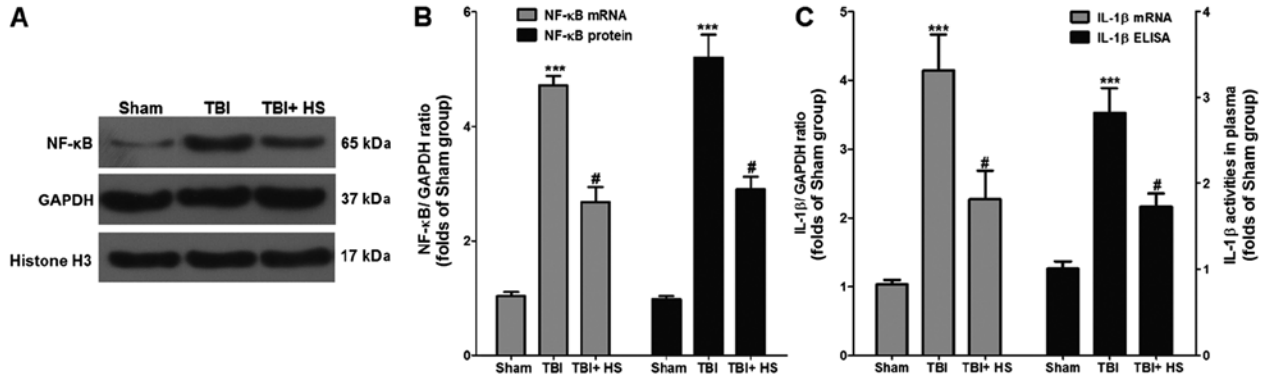

Figure 6. HS treatment reduces TBI-induced inflammation. (A) NF-κB protein expression in cerebral cortical tissues around the contusion site was determined by western blotting. (B) Quantitative analysis of NF-κB mRNA and protein expression levels in each group. (C) Plasma IL-1β concentrations and the tissue mRNA expression of IL-1β were evaluated by ELISA and reverse transcription-quantitative PCR, respectively. Data are presented as the mean ± SD. $^{\#}$P<0.05 vs. TBI group. ***P<0.001 vs. the sham group. TBI, traumatic brain injury; HS, hypertonic saline; IL, interleukin.

sion levels of AQP 4 are upregulated in swollen glial cells in the cerebrum and the contusion area. Sun *et al* (32) also showed that brain edema in rats reaches a peak 24 h following TBI modeling, where AQP4 expression in astrocytes in the injury area was significantly enhanced, whilst that in the peripheral area is weakened compared with the injury area and AQP4 expression in other areas remained unchanged. Yao *et al* (11) also reported that AQP4 knockout can evidently reduce brain edema and injury in cerebral ischemia mice. In AQP4 knockdown mice, improved outcomes could be achieved after TBI by reducing cytotoxic brain water accumulation (33). Furthermore, AER-271, an AQP4 inhibitor, has been previously demonstrated to block acute brain edema, whilst improving the short-term outcomes of a rat pediatric asphyxia cardiac arrest model (34). Previous studies have also indicated that AQP4 deletion in mice can reduce neuronal death and brain edema following acute ischemic stroke and water intoxication (35,36). Therefore, suppressing AQP4 at an appropriate time can reduce the accumulation of edema fluid in the brain, thus lowering morbidity and mortality. The present results also indicated that HS can be applied to treat TBI-induced brain edema, with this effect is closely associated with the suppression of AQP4.

TBI-induced brain edema involves a highly complex mechanism, where the destruction of BBB integrity is an important link between vasogenic brain edema and secondary injuries (37). TJ proteins, consisting of the transmembrane complex (occludins and claudins) and cytoplasmic (ZO family) proteins, are anchored to the actin cytoskeleton and are markers of BBB integrity, which contribute to its structural strength (38). It has been reported in both animal and human TBI studies that increased BBB permeability contributes to the pathophysiology of brain edema, which may be caused by increased BBB permeability via the degradation of TJ proteins, including claudin-5, occludin and ZO-1 (39,40). In addition, AQP4 expression is abundant in structures associated with the BBB, including the foot processes of astrocytes and the basolateral plasma membrane of the ependymal epithelium (9). A previous study has also revealed that AQP 4 content is closely associated with the integrity of the BBB (41). The present study also suggested that albumin expression in post-TBI tissues was significantly increased, suggesting that the BBB was compromised, whilst HS treatment restored BBB integrity in rats.

The activation of astrocytes is mainly characterized by cell body hypertrophy of astrocytes with the notable thickening of protrusions (42). Additionally, it has been previously reported that astrocyte activation is a common stress response in the CNS under numerous pathological conditions (43). In the present study, IHC staining suggested that the expression of GFAP was enhanced. A previous study also revealed that 6 h after brain trauma, astrocytes were found to be activated in the cortex around the injury site, where additional reactive astrocytes were found in the entire injured hemisphere at 24 h and were more pronounced than at 72 h (44). In another study, activated astrocytes were previously observed in the hippocampus 24 h, 3 and 7 days after brain injury, but the number of activated astrocytes was not significantly changed (45). The present study indicated that 2 days after TBI, GFAP expression was significantly elevated, suggesting that astrocytes were activated, which was reversed by HS treatment. However, the dynamic changes that occur in astrocytes during HS treatment require further investigation.

Elevated inflammation is characteristic of brain edema, such that brain edema formation and posttraumatic inflammation are two key pathological processes that are associated with secondary brain injury (46). According to a previous study, 10% HS could alleviate brain edema by inhibiting the Na-K-2Cl co-transporter isoform 1 (NKCC1), where this process was found to be mechanistically due to the attenuation of NKCC1 stimulation by IL-1β and TNF-α (47). Previous studies have also reported the relationship between inflammation and brain edema. Holmin and Mathiesen (48) revealed that intraventricular injection of TNF-α and IL-1β, or the injection of TNF-α into swine through the internal carotid artery can induce an inflammatory response in the brain and increase BBB permeability in the brain cortex, thus inducing vasogenic brain edema. In addition, Ito *et al* (49) showed that the lateral intraventricular injection of IL-1β can induce AQP4 expression in brain tissue in rats and that an inhibitor can suppress the induction of astrocyte expression *in vitro*, suggesting the possible participation of IL-1β in brain edema formation via the activation of astrocytes through the induction pathway. In addition, a previous study revealed that suppressing IL-1β

can mitigate TBI and brain edema and improve behaviors associated with depression in rats after brain injury (50). In the present study, it was demonstrated that the effect of HS on brain edema resulting from TBI was closely associated with reductions in the levels of TBI-induced inflammatory factors.

NF-κB serves as a key player in the neuroinflammatory response in astrocytes during various neurological disorders by promoting the transcription of inflammatory mediators, including proinflammatory cytokines and chemokines (51). IL-1β can be triggered by binding to the receptor IL-1R, which is an upstream signaling factor of NF-κB (52). It has also been demonstrated that IL-1β can increase BBB permeability and disruption by downregulating the expression of TJ proteins (53). A recent study also revealed that inhibiting NF-κB binding activity and translocation can reduce inflammatory cell infiltration, reduce matrix metalloproteinase-9 expression and ameliorating BBB disruption (54). The present results suggested that HS treatment inhibited NF-κB, IL-1β and BBB permeability, but no direct evidence regarding the relationship between NF-κB/IL-1β and BBB function as a result of HS treatment of brain edema was identified, which require further study.

However, some limitations associated with the current study should be noted. Firstly, the present study only evaluated brain edema at the end point of the experiments using T2WI. Therefore, monitoring of the progression of brain edema through different MRI sequences should be addressed in future studies. Additionally, although previous studies have reported cell death after TBI (55,56), the present study did not evaluate parameters of cell death, including that of neurons and various types of glial cells, since it was mainly focused on brain edema during TBI and HS treatment. Therefore, future studies should focus on the mechanism of cell apoptosis in TBI. Another limitation of the present study was that the treatment effect of only one dose (10%) of HS on brain edema was evaluated. Increased attention should be provided to the effects of different concentrations of HS to identify the optimal treatment conditions for different types of brain edema in future studies.

In conclusion, the present study identified the protective effect of tail vein injections of HS in a rat model of TBI-induced brain edema via MRI, BWC detection and histology. It was demonstrated that HS significantly reduced the upregulated expression of AQP4 induced by TBI. Further analysis of inflammatory factors suggested that the efficacy of HS in brain edema resulting from TBI was closely related to the downregulation of AQP4, the restoration of BBB integrity and the suppression of inflammatory factors IL-1β and NF-κB. However, the precise regulatory mechanism remains to be further elucidated.

Acknowledgements

Not applicable.

Funding

This work was supported by Projects of medical and health technology development program in Shandong province (grant no. 2017WS037).

Availability of data and materials

The datasets used and/or analyzed during the current study are available from the corresponding author on reasonable request.

Authors' contributions

HZ performed animal experiments and prepared this manuscript. JL performed the MRI experiment. YL performed the H&E and IHC experiments. CS measured the BWC. GF performed molecular biology experiments. WL performed statistical analysis. LF designed this study and was a major contributor in writing the manuscript. All authors read and approved the final manuscript.

Ethics approval and consent to participate

All of the animal procedures were conducted in accordance with the Guidelines for Care and Use of Laboratory Animals, and were approved by the Animal Care and Use Committee at Jining No. 1 People's Hospital (approval no. 2017037).

Patient consent for publication

Not Applicable

Competing interests

The authors declare that they have no competing interests.

References

1. Capizzi A, Woo J and Verduzco-Gutierrez M: Traumatic brain injury: An overview of epidemiology, pathophysiology, and medical management. Med Clin North Am 104: 213-238, 2020.
2. Honeybul S: Reconsidering the role of hypothermia in management of severe traumatic brain injury. J Clin Neurosci 28: 12-15, 2016.
3. Donkin JJ and Vink R: Mechanisms of cerebral edema in traumatic brain injury: Therapeutic developments. Curr Opin Neurol 23: 293-299, 2010.
4. Adeva MM, Souto G, Donapetry C, Portals M, Rodriguez A and Lamas D: Brain edema in diseases of different etiology. Neurochem Int 61: 166-174, 2012.
5. Kochanek PM, Jackson TC, Ferguson NM, Carlson SW, Simon DW, Brockman EC, Ji J, Bayır H, Poloyac SM, Wagner AK, *et al*: Emerging therapies in traumatic brain injury. Semin Neurol 35: 83-100, 2015.
6. Mamtilahun M, Tang G, Zhang Z, Wang Y, Tang Y and Yang GY: Targeting Water in the Brain: Role of Aquaporin-4 in Ischemic Brain Edema. Curr Drug Targets 20: 748-755, 2019.
7. Kitchen P, Day RE, Salman MM, Conner MT, Bill RM and Conner AC: Beyond water homeostasis: Diverse functional roles of mammalian aquaporins. Biochim Biophys Acta 1850: 2410-2421, 2015.
8. Verkman AS, Anderson MO and Papadopoulos MC: Aquaporins: Important but elusive drug targets. Nat Rev Drug Discov 13: 259-277, 2014.
9. Papadopoulos MC and Verkman AS: Aquaporin water channels in the nervous system. Nat Rev Neurosci 14: 265-277, 2013.
10. Papadopoulos MC, Manley GT, Krishna S and Verkman AS: Aquaporin-4 facilitates reabsorption of excess fluid in vasogenic brain edema. FASEB J 18: 1291-1293, 2004.
11. Yao X, Derugin N, Manley GT and Verkman AS: Reduced brain edema and infarct volume in aquaporin-4 deficient mice after transient focal cerebral ischemia. Neurosci Lett 584: 368-372, 2015.
12. Liu S, Mao J, Wang T and Fu X: Downregulation of Aquaporin-4 protects brain against hypoxia ischemia via anti-inflammatory mechanism. Mol Neurobiol 54: 6426-6435, 2017.

13. Yin J, Zhang H, Chen H, Lv Q and Jin X: Hypertonic Saline Alleviates Brain Edema After Traumatic Brain Injury via Downregulation of Aquaporin 4 in Rats. Med Sci Monit 24: 1863-1870, 2018.
14. National Research Council (US) Committee for the Update of the Guide for the Care and Use of Laboratory Animals: Guide for the Care and Use of Laboratory Animals. 8th edition. National Academies Press (US), Washington (DC), 2011.
15. Huang L, Cao W, Deng Y, Zhu G, Han Y and Zeng H: Hypertonic saline alleviates experimentally induced cerebral oedema through suppression of vascular endothelial growth factor and its receptor VEGFR2 expression in astrocytes. BMC Neurosci 17: 64, 2016.
16. Wen M, Ye J, Han Y, Huang L, Yang H, Jiang W, Chen S, Zhong W, Zeng H and Li DY: Hypertonic saline regulates microglial M2 polarization via miR-200b/KLF4 in cerebral edema treatment. Biochem Biophys Res Commun 499: 345-353, 2018.
17. Niu F, Dong J, Xu X, Zhang B and Liu B: Mitochondrial division inhibitor 1 prevents early-stage induction of mitophagy and accelerated cell death in a rat model of moderate controlled cortical impact brain injury. World Neurosurg 122: e1090-e1101, 2019.
18. Paxinos G and Watson C: The rat brain in stereotaxic coordinates. 6th Edition. Elsevier, 2007.
19. Gerriets T, Stolz E, Walberer M, Müller C, Kluge A, Bachmann A, Fisher M, Kaps M and Bachmann G: Noninvasive quantification of brain edema and the space-occupying effect in rat stroke models using magnetic resonance imaging. Stroke 35: 566-571, 2004.
20. Zhao M, Liang F, Xu H, Yan W and Zhang J: Methylene blue exerts a neuroprotective effect against traumatic brain injury by promoting autophagy and inhibiting microglial activation. Mol Med Rep 13: 13-20, 2016.
21. Khaksari M, Soltani Z, Shahrokhi N, Moshtaghi G and Asadikaram G: The role of estrogen and progesterone, administered alone and in combination, in modulating cytokine concentration following traumatic brain injury. Can J Physiol Pharmacol 89: 31-40, 2011.
22. Li W, Wang R, Xie H, Zhang J and Jia Z: Changes of pathological and physiological indicators affecting drug metabolism in rats after acute exposure to high altitude. Exp Ther Med 9: 98-104, 2015.
23. Livak KJ and Schmittgen TD: Analysis of relative gene expression data using real-time quantitative PCR and the 2(-Delta Delta C(T)) Method. Methods 25: 402-408, 2001.
24. Stokum JA, Kurland DB, Gerzanich V and Simard JM: Mechanisms of astrocyte-mediated cerebral edema. Neurochem Res 40: 317-328, 2015.
25. Kimelberg HK: Current concepts of brain edema. Review of laboratory investigations. J Neurosurg 83: 1051-1059, 1995.
26. Hatashita S, Hoff JT and Salamat SM: Ischemic brain edema and the osmotic gradient between blood and brain. J Cereb Blood Flow Metab 8: 552-559, 1988.
27. Wasterlain CG and Torack RM: Cerebral edema in water intoxication. II. An ultrastructural study. Arch Neurol 19: 79-87, 1968.
28. Hara-Chikuma M and Verkman AS: Physiological roles of glycerol-transporting aquaporins: The aquaglyceroporins. Cell Mol Life Sci 63: 1386-1392, 2006.
29. Papadopoulos MC and Verkman AS: Aquaporin-4 gene disruption in mice reduces brain swelling and mortality in pneumococcal meningitis. J Biol Chem 280: 13906-13912, 2005.
30. Appelboom G, Bruce S, Duren A, Piazza M, Monahan A, Christophe B, Zoller S, LoPresti M and Connolly ES: Aquaporin-4 gene variant independently associated with oedema after intracerebral haemorrhage. Neurol Res 37: 657-661, 2015.
31. Suzuki R, Okuda M, Asai J, Nagashima G, Itokawa H, Matsunaga A, Fujimoto T and Suzuki T: Astrocytes co-express aquaporin-1, -4, and vascular endothelial growth factor in brain edema tissue associated with brain contusion. Acta Neurochir Suppl (Wien) 96: 398-401, 2006.
32. Sun MC, Honey CR, Berk C, Wong NL and Tsui JK: Regulation of aquaporin-4 in a traumatic brain injury model in rats. J Neurosurg 98: 565-569, 2003.
33. Yao X, Uchida K, Papadopoulos MC, Zador Z, Manley GT and Verkman AS: Mildly reduced brain swelling and improved neurological outcome in aquaporin-4 knockout mice following controlled cortical impact brain injury. J Neurotrauma 32: 1458-1464, 2015.
34. Wallisch JS, Janesko-Feldman K, Alexander H, Jha RM, Farr GW, McGuirk PR, Kline AE, Jackson TC, Pelletier MF, Clark RSB, *et al*: The aquaporin-4 inhibitor AER-271 blocks acute cerebral edema and improves early outcome in a pediatric model of asphyxial cardiac arrest. Pediatr Res 85: 511-517, 2019.
35. Manley GT, Fujimura M, Ma T, Noshita N, Filiz F, Bollen AW, Chan P and Verkman AS: Aquaporin-4 deletion in mice reduces brain edema after acute water intoxication and ischemic stroke. Nat Med 6: 159-163, 2000.
36. Katada R, Akdemir G, Asavapanumas N, Ratelade J, Zhang H and Verkman A: Greatly improved survival and neuroprotection in aquaporin-4-knockout mice following global cerebral ischemia. FASEB J 28: 705-714, 2014.
37. Jha RM, Kochanek PM and Simard JM: Pathophysiology and treatment of cerebral edema in traumatic brain injury. Neuropharmacology 145 (Pt B): 230-246, 2019.
38. Alves JL: Blood-brain barrier and traumatic brain injury. J Neurosci Res 92: 141-147, 2014.
39. Lu L, Wang M, Yuan F, Wei X and Li W: Roles of elevated 20 HETE in the breakdown of blood brain barrier and the severity of brain edema in experimental traumatic brain injury. Mol Med Rep 17: 7339-7345, 2018.
40. Kim JY, Ko AR, Hyun HW and Kang TC: ETB receptor-mediated MMP-9 activation induces vasogenic edema via ZO-1 protein degradation following status epilepticus. Neuroscience 304: 355-367, 2015.
41. Nico B, Frigeri A, Nicchia GP, Quondamatteo F, Herken R, Errede M, Ribatti D, Svelto M and Roncali L: Role of aquaporin-4 water channel in the development and integrity of the blood-brain barrier. J Cell Sci 114: 1297-1307, 2001.
42. Escartin C and Bonvento G: Targeted activation of astrocytes: A potential neuroprotective strategy. Mol Neurobiol 38: 231-241, 2008.
43. Hol EM and Pekny M: Glial fibrillary acidic protein (GFAP) and the astrocyte intermediate filament system in diseases of the central nervous system. Curr Opin Cell Biol 32: 121-130, 2015.
44. Okimura Y, Tanno H, Fukuda K, Ohga M, Nakamura M, Aihara N and Yamaura A: Reactive astrocytes in acute stage after experimental brain injury: Relationship to extravasated plasma protein and expression of heat shock protein. J Neurotrauma 13: 385-393, 1996.
45. Burda JE, Bernstein AM and Sofroniew MV: Astrocyte roles in traumatic brain injury. Exp Neurol 275: 305-315, 2016.
46. Hopp S, Nolte MW, Stetter C, Kleinschnitz C, Sirén AL and Albert-Weissenberger C: Alleviation of secondary brain injury, posttraumatic inflammation, and brain edema formation by inhibition of factor XIIa. J Neuroinflammation 14: 39, 2017.
47. Huang LQ, Zhu GF, Deng YY, Jiang WQ, Fang M, Chen CB, Cao W, Wen MY, Han YL and Zeng HK: Hypertonic saline alleviates cerebral edema by inhibiting microglia-derived TNF-α and IL-1β-induced Na-K-Cl Cotransporter up-regulation. J Neuroinflammation 11: 102, 2014.
48. Holmin S and Mathiesen T: Intracerebral administration of interleukin-1beta and induction of inflammation, apoptosis, and vasogenic edema. J Neurosurg 92: 108-120, 2000.
49. Ito H, Yamamoto N, Arima H, Hirate H, Morishima T, Umenishi F, Tada T, Asai K, Katsuya H and Sobue K: Interleukin-1beta induces the expression of aquaporin-4 through a nuclear factor-kappaB pathway in rat astrocytes. J Neurochem 99: 107-118, 2006.
50. Fenn AM, Skendelas JP, Moussa DN, Muccigrosso MM, Popovich PG, Lifshitz J, Eiferman DS and Godbout JP: Methylene blue attenuates traumatic brain injury-associated neuroinflammation and acute depressive-like behavior in mice. J Neurotrauma 32: 127-138, 2015.
51. Skaper SD, Facci L, Zusso M and Giusti P: An inflammation-centric view of neurological disease: Beyond the neuron. Front Cell Neurosci 12: 72, 2018.
52. Liu R, Pan MX, Tang JC, Zhang Y, Liao HB, Zhuang Y, Zhao D and Wan Q: Role of neuroinflammation in ischemic stroke. Neuroimmunol Neuroinflamm 4: 158-166, 2017.
53. Blamire AM, Anthony DC, Rajagopalan B, Sibson NR, Perry VH and Styles P: Interleukin-1β -induced changes in blood-brain barrier permeability, apparent diffusion coefficient, and cerebral blood volume in the rat brain: A magnetic resonance study. J Neurosci 20: 8153-8159, 2000.
54. Lee WT, Tai SH, Lin YW, Wu TS and Lee EJ: YC 1 reduces inflammatory responses by inhibiting nuclear factor κB translocation in mice subjected to transient focal cerebral ischemia. Mol Med Rep 18: 2043-2051, 2018.
55. Sater AP, Rael LT, Tanner AH, Lieser MJ, Acuna DL, Mains CW and Bar-Or D: Cell death after traumatic brain injury: Detrimental role of anoikis in healing. Clin Chim Acta 482: 149-154, 2018.
56. Raghupathi R: Cell death mechanisms following traumatic brain injury. Brain Pathol 14: 215-222, 2004.